Chemical Reaction Studies in CH_4/Ar and CH_4/N_2 Gas Mixtures of a Dielectric Barrier Discharge

Abhijit Majumdar, Jürgen F. Behnke, and Rainer Hippler*

Institut für Physik, Ernst-Moritz-Arndt-Universität Greifswald, Domstrasse 10a, 17489 Greifswald, Germany

Konstantin Matyash and Ralf Schneider

Max-Planck-Institut für Plasmaphysik, EURATOM Association, Wendelsteinstraβe 1, 17491 Greifswald, Germany

Received: June 30, 2005; In Final Form: August 22, 2005

Chemical reactions in a dielectric barrier discharge at medium pressure of 250−300 mbar have been studied in CH_4/Ar and CH_4/N_2 gas mixtures by means of mass spectrometry. The main reaction scheme is production of H_2 by fragmentation of CH_4, but also production of higher order hydrocarbon molecules such as C_nH_m with n up to 9 including formation of different functional CN groups is observed. Formation of C_2H_2, C_2H_4, and C_2H_6 molecules has been investigated in some detail. Significant differences are noted in comparison to a theoretical estimate.

I. Introduction

Atmospheric pressure dielectric barrier discharges (DBD) are of great interest for application in, e.g., gas chemistry, sterilization, surface activation, and modification or thin film deposition.[1−5] The development of a new process based on this discharge needs a clear understanding of plasma and discharge physics and chemistry. At the present time much attention is paid to the chemical processes in barrier discharge plasma in various gas mixtures, since the understanding of these processes is necessary for the development of industrial reactors.[6−8] We have chosen a gas mixture of CH_4/N_2 with a gas ratio of 1:2 to investigate physical properties and chemical efficiency of barrier discharges. Nitrogen and methane are abundantly available in the Earth's and particularly in Titan's atmosphere and thus play an important role in atmospheric plasma chemistry.[9] Furthermore, Ar- and N_2-containing plasmas are more stable to operate than a pure CH_4 plasma. Hence, a mixture of CH_4 and N_2 or Ar offers stable plasma conditions. Industrial applications of CH_4/N_2 and CH_4/Ar gas mixtures under consideration here are production of hydrogen and of higher order hydrocarbon molecules having applications in polymer industries and fundamental plasma chemistry. Moreover, such composition can result in unexpected changes in the physical properties of the discharge itself and can turn into a strong influence on the formation of plasma chemical products.[10] The aim of this work is to study discharge properties of CH_4/N_2 and CH_4/Ar gas mixtures in a high voltage dielectric barrier discharge (DBD) medium, the influence of the plasma on organic gases, and interpretation of the experimental results.

II. Experiment Section

The experimental set up is shown in Figure 1. The plasma chamber is made of stainless steel. The inner dimensions of the chamber are height 12.3 cm, length 18.0 cm, and width 15.0 cm, yielding a chamber volume of 3.32 dm^3. The two electrodes are made from Ag plates with a length of 8.3 cm, width 3.3 cm, and thickness 0.15 cm. Both Ag electrodes are covered by dielectrics: the upper (powered) electrode is covered with aluminum oxide ($\epsilon \approx 10$); the lower (grounded) electrode with a glass plate ($\epsilon = 3.8$). Both electrodes are separated by 0.15 cm from each other. The upper electrode is connected to a home-built high voltage power supply, while the lower electrode is grounded. The chamber is pumped by a membrane pump down to about 10 mbar. Pressure inside the plasma chamber was controlled by two gas flow controllers for methane and nitrogen and by an adjustable needle valve between the chamber and the membrane pump. The experiments were performed with the chamber filled at a pressure of 250−300 mbar and with pump and gas flow shut off.

The high voltage power supply consists of a frequency generator delivering a sinusoidal output that is fed into an audio amplifier. The amplifier can be operated at up to 500 W; its output is fed into a spark plug transformer. Experiments were performed at 10.5 kV (peak-to-peak) and at 5.5 kHz. The electrical power under these conditions was 5 W. It was measured by placing a probe capacitor (10 nF) between the lower electrode and ground and measuring the collected charge together with the applied voltage as function of time, as described by Wagner et al. and Sonnenfeld et al.[5,11]

Gas composition of stable reaction products only was detected by a mass spectrometer (Balzers QMS 200). It is pumped by a turbomolecular pump (Pfeiffer TSU 062H) to a base pressure of about 1×10^{-8} mbar increasing to about 10^{-6} mbar during the experiment. A capillary tube of length 103 cm and inner diameter 0.01 cm connects the mass spectrometer with the plasma chamber. A pressure of 10^{-2} mbar at the entrance to the mass spectrometer is maintained during the experiments with the help of a second turbomolecular pump (Balzers 071P).

Figure 2 shows two typical mass spectra in the range of mass numbers up to $m/z = 140$ that were obtained after the chamber has been filled with 250 mbar of a CH_4/N_2 gas mixture (mixing ratio 1:2). Figure 2a represents the initial gas composition

* To whom correspondence should be addressed. E-mail: hippler@physik.uni-greifswald.de.

10.1021/jp053588a CCC: $30.25
Published on Web 09/28/2005

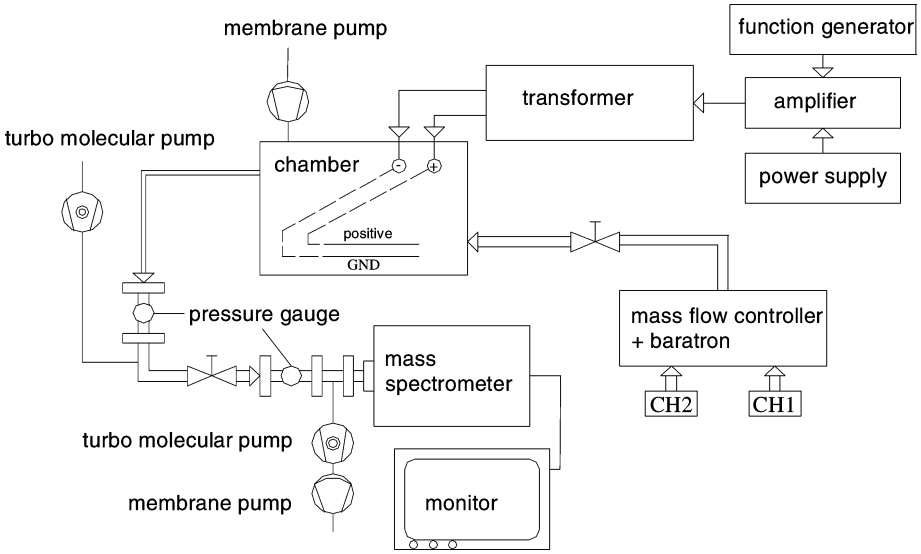

Figure 1. Experimental setup (schematic).

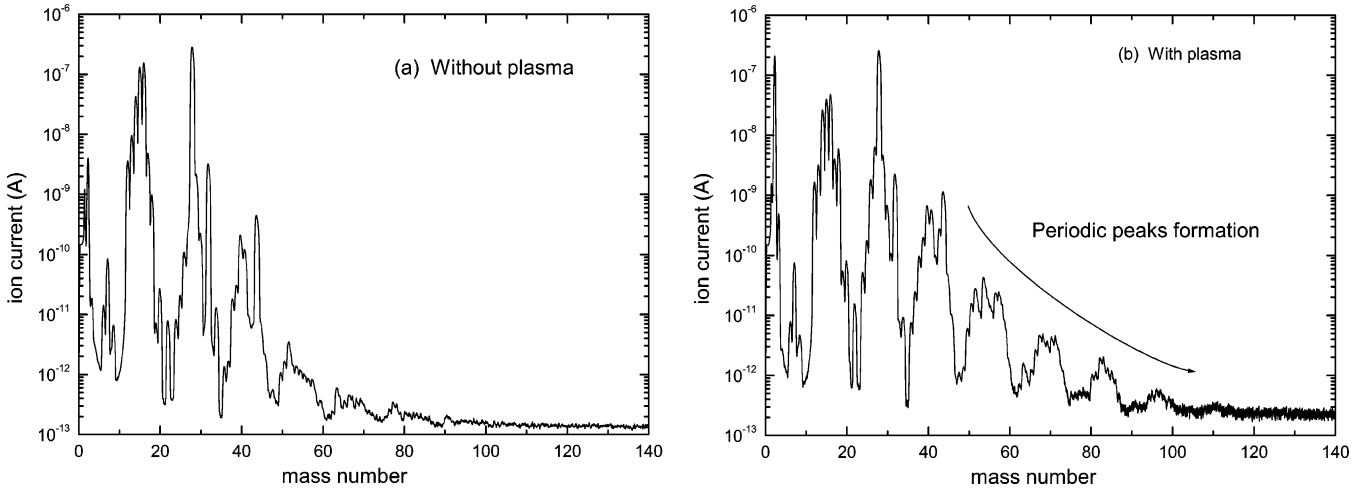

Figure 2. Mass spectra obtained from a CH_4/N_2 gas mixture (a) without plasma and (b) after 640 min with the plasma on.

consisting of nitrogen (N_2) and methane (CH_4) gas. Impurities that are present consist, e.g., of oxygen (O_2) and small amounts of higher hydrocarbons around mass numbers $m/z = 40$, 55, 65, and 78. It should be noted that stable molecules dissociate inside the ion source of the mass spectrometer, giving rise to the formation of unstable radical ions that complicate the data analysis.[12,13] For example, methane shows up in the mass spectra with masses $m/z = 16$ (CH_4^+), 15 (CH_3^+), 14 (CH_2^+), 13 (CH^+), and even 12 (C^+).

Figure 2b displays the mass spectrum obtained from the same gas after the discharge has been operated for 570 min. Several differences compared to Figure 2a are noted: (i) a reduction of the methane peaks, (ii) an increase of the hydrogen peak, and (iii) the appearance of higher hydrocarbon peaks. The experimental results presented below are obtained by subtracting the mass spectra obtained without plasma from those obtained with plasma, e.g, by subtracting the data of Figure 2a from those of Figure 2b.

To accurately determine the mass number of the detected species we have carried out a mass calibration employing H_2, CH_4, N_2, Ar, Xe, and SF_6 gases. The results are shown in Figure 3 where the displayed mass number m/z is plotted versus the correct mass number m_0/z. Small deviations amounting to up to about one mass number around 100 amu are noted and have been taken into account in the assignment of the observed species.

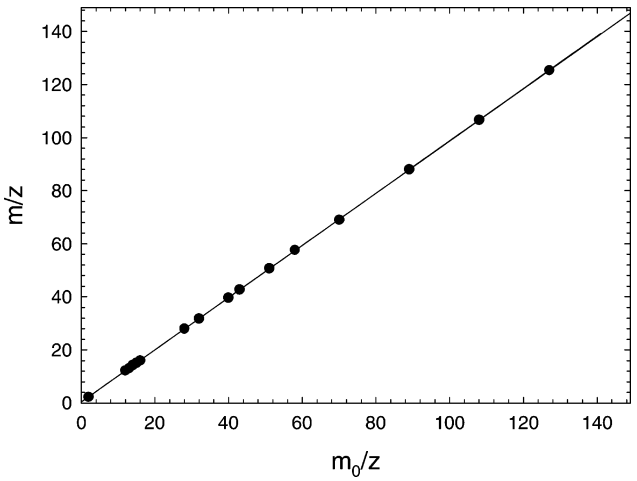

Figure 3. The displayed mass number m/z versus the correct mass number m_0/z. The solid line is a least-squares fit yielding $m/z = 0.2711 + 0.9853\ m_0/z$.

To compare the hydrogen (H_2) and methane (CH_4) signals a relative sensitivity calibration was performed. This was done by filling the chamber with 240 mbar of either Ar/CH_4 or N_2/CH_4 gas mixture (mixing ratio 1:2) and with 20−100 mbar of H_2. A linear increase of the hydrogen signal with increasing hydrogen partial pressure is noted (Figure 4). At the same time,

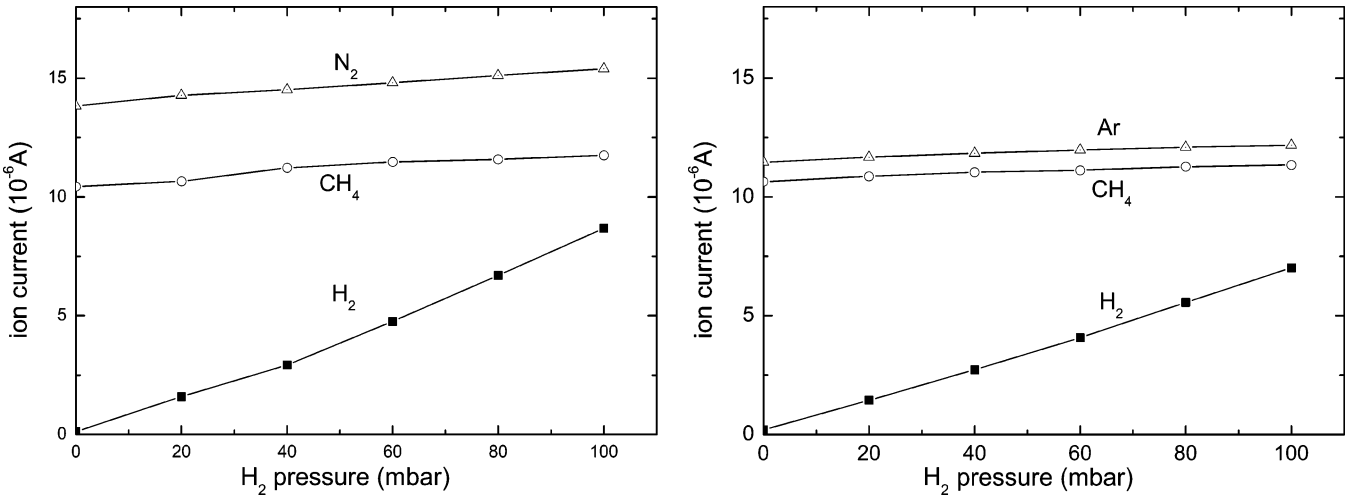

Figure 4. The measured H_2 ($m/z = 2$), CH_4 ($m/z = 15-16$), and N_2 ($m/z = 28$) respective Ar ion signal versus hydrogen partial pressure for the two $N_2/CH_4/H_2$ and $Ar/CH_4/H_2$ gas mixtures (see text).

the signals from the other two gases remain approximately constant. Form the measurements we may extract the relative sensitivity $\epsilon(H_2)/\epsilon(CH_4)$ of hydrogen relative to methane for the investigated gas mixtures. We obtain $\epsilon(H_2)/\epsilon(CH_4) = 0.58$ and $\epsilon(H_2)/\epsilon(CH_4) = 0.56$ for the $N_2/CH_4/H_2$ and $Ar/CH_4/H_2$ gas mixtures, respectively.

III. Particle Balance

To estimate the hydrocarbon species distribution in the experimental we employ a zero-dimensional particle-balance model as has been used recently.[14] In this model we assume that the plasma is uniform, electrons and ions have a Maxwellian energy distribution, and electron temperature and density and ion temperature are constant. What we are aiming for with this model are the temporal behavior of neutral and ion species densities. We assume that they change only due to volume chemical reactions, external sources, and pumping. In this case, all species densities are governed by the system of particle-balance equations

$$\frac{dn_\alpha}{dt} = \sum R^\alpha_{\beta\gamma} n_\beta n_\gamma - n_\alpha \sum R^\beta_{\alpha\gamma} n_\gamma + S_\alpha - P_\alpha \qquad (1)$$

with

$$R^\alpha_{\beta\gamma} = \int_{v\beta} \int_{v\gamma} \sigma^\alpha_{\beta\gamma}(E_{\beta\gamma})\, \vec{u}_{\beta\gamma}\, f_\beta(\vec{v}_\beta)\, f_\gamma(\vec{v}_\gamma)\, d^3v_\beta\, d^3v_\gamma \qquad (2)$$

is the rate coefficient for volume reaction between species β and γ, leading to the creation of species α, $\sigma^\alpha_{\beta\gamma}(E_{\beta\gamma})$ is the cross-section of this process, which depends on the center-of-mass energy $E_{\beta\gamma} = \mu_{\beta\gamma} u^2_{\beta\gamma}/2$ of colliding particles, $\vec{u}_{\beta\gamma} = \vec{v}_\beta - \vec{v}_\gamma$ is the relative velocity, $\mu_{\beta\gamma} = m_\beta m_\gamma/(m_\beta + m_\gamma)$ is the effective mass of the particles, $f_\beta(\vec{v}_\beta)$ is the distribution function of particle β, n_α is the density of species α, S_α is the volume source, and P_α is the volume pumping rate of species α. To compare with the present experiment (without gas flow) we use $S_\alpha = P_\alpha = 0$. As we consider the electron density to be constant, to maintain quasi-neutrality we multiply ion densities by a factor $n_e/\sum_k n_{i_k}$ at every time step. In our model we account for 174 volume reactions involving 14 neutral and 13 charged species: C_2H_6, C_2H_5, C_2H_4, C_2H_3, C_2H_2, C_2H, C_2, CH_4, CH_3, CH_2, CH, C, H_2, H, and $C_2H_5^+$, $C_2H_4^+$, $C_2H_3^+$, $C_2H_2^+$, C_2H^+, CH_4^+, CH_3^+, CH_2^+, CH^+, C^+, H_2^+, and H^+.

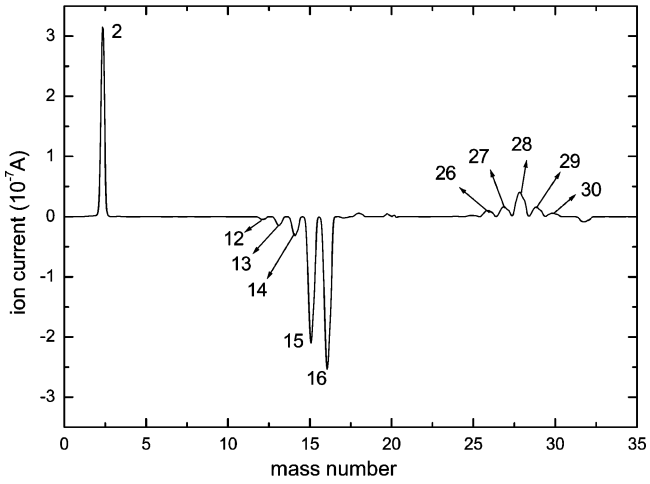

Figure 5. Difference mass spectrum with and without plasma in the mass range m/z up to 35 for a CH_4/Ar gas mixture. Note the linear scale. Also note that labels refer to detected ions which may be fragments of larger parent molecules.

The number of reactions considered was determined by the available data for reaction rate coefficients. For reaction rate coefficients of electron and proton induced methane break-up, we used well-known Ehrhardt−Langer analytical fits.[15] For ion−neutral, neutral−neutral hydrocarbon reactions and electron-impact reactions for hydrocarbons higher than CH_4, we used constant rate coefficients from data sets used by Riccardi et al.[16] and Herrebout et al.[17]

IV. Results

In the following we separately present our results for the two CH_4/Ar and CH_4/N_2 gas mixtures.

A. CH_4/Ar. Figure 5 displays the measured difference spectrum for mass numbers up to $m/z = 35$ on a linear scale obtained by subtracting the data without plasma from those obtained with plasma. From Figure 5 the production of a large amount of hydrogen (H_2) and a significant consumption of methane, the latter corroborated by the (negative) methane peaks ($m/z = 12-16$), becomes evident. In addition, production of a significant amount of C_2H_m molecules ($m/z = 26-30$) becomes evident. The difference spectrum in the mass range $m/z = 20-140$ is displayed in Figure 6 on a logarithmic scale. The broad prominent peaks, each composed of several individual peaks, are attributed to C_nH_m molecules with n up to 9 and $m \approx$

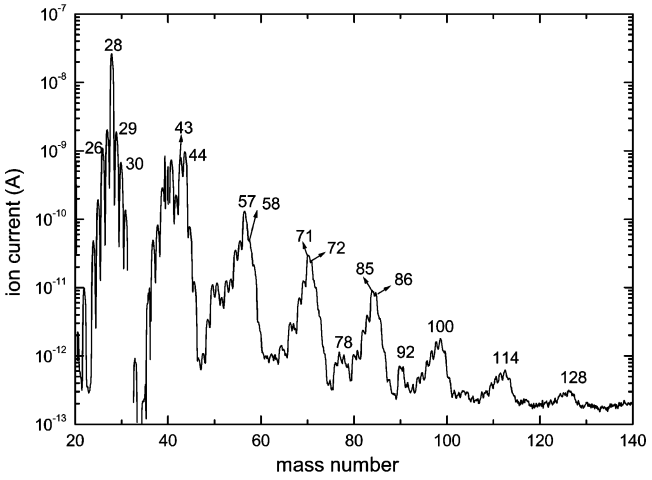

Figure 6. Difference mass spectrum with and without plasma in the mass range $m/z = 20-140$ for a CH_4/Ar gas mixture.

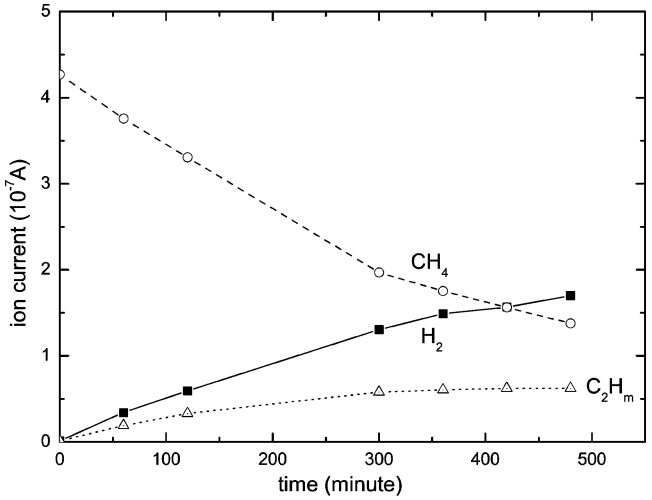

Figure 7. Time dependence of the hydrogen ($m/z = 2$), methane ($m/z = 12-16$), and summed C_2H_m ($m/z = 26$, 28, 30) peaks in the CH_4/Ar gas mixture.

$2n + 2$. The most prominent peaks, hence, approximately differ by $m/z \approx 14$ from each other. Evidently, one CH_2 radical is adding up in consecutive reactions and in consequence the spectrum becomes periodic.

The origin of the mass peak at $m/z = 29$ is, in addition, attributed to a C_2H_5 fragment of larger hydrocarbon molecules, e.g., C_3H_8 ($m/z = 44$) and C_4H_{10} ($m/z = 58$), also present in the mass spectrum. Other prominent peaks in the spectrum occurring at $m/z = 72$, 86, 100, 114, and 128 are attributed to the large alkane molecules C_5H_{12}, C_6H_{14}, C_7H_{16}, C_8H_{18}, and C_9H_{20}, respectively. It should be emphasized that large molecules break-up during ionization and it is rather common for detected fragment ions to differ by, e.g, a CH_3 or C_2H_5 group from the unfragmented parent molecule. There is some evidence for formation of cyclic molecules, as is inferred from the mass peaks at $m/z = 78$ and 92 which may be attributed to cyclic benzene (C_6H_6) and methyl-benzene ($CH_3-C_6H_5$), respectively, and/or for the formation of the chain hexadiyne and heptadiyne molecules.

The time dependence of the H_2, CH_4, and higher C_2H_m ($m = 2$, 4, 6) mass peaks is shown in Figures 7 and 8. While the hydrogen and the C_2H_m peaks show a pronounced increase, the summed methane peaks ($m/z = 12-16$) follow an approximately exponential decay. About 75% of the total methane is consumed within 500 min; it corresponds to an energy consumption of

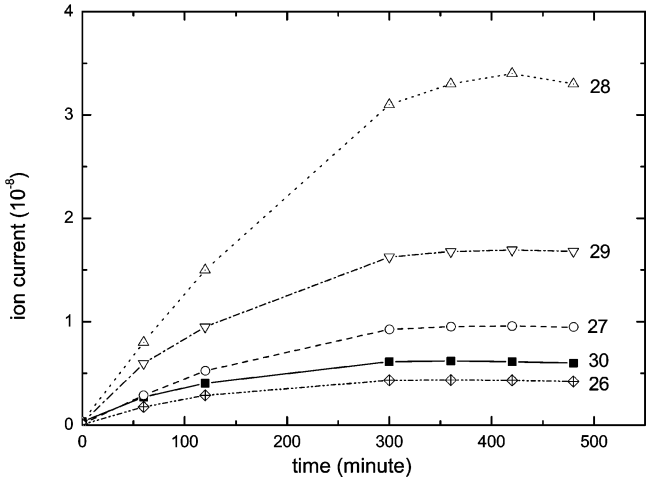

Figure 8. Time dependence of the $C_2H_2^+$ ($m/z = 26$), $C_2H_3^+$ ($m/z = 27$), $C_2H_4^+$ ($m/z = 28$), $C_2H_5^+$ ($m/z = 29$), and $C_2H_6^+$ ($m/z = 30$) ion mass peaks in the CH_4/Ar gas mixture.

TABLE 1: Relative Intensities of the Fragmentation Pattern of C_2H_2, C_2H_4, and C_2H_6 at $m/z = 25-30$, According to Ref 18

m/z	25	26	27	28	29	30
C_2H_2	0.167	0.833	-	-	-	-
C_2H_4	0.033	0.235	0.254	0.469	-	-
C_2H_6	-	0.122	0.176	0.488	0.102	0.112

about 50 eV per consumed methane molecule or 4800 kJ/mol. Taking into account the relative detection efficiency of hydrogen ($\epsilon \simeq 0.56$) with respect to methane we note that consumption of a methane molecule contributes to the formation of an hydrogen molecule roughly on a one-to-one basis. Decomposition of methane leading to the formation of hydrogen molecules is, hence, the dominant chemical reaction in the plasma. Furthermore, it appears that within experimental errors every consumed methane molecule contributes to the formation of an hydrogen molecule, i.e., a gross reaction scheme

$$CH_4 \rightarrow CH_2 + H_2 \tag{3}$$

which may include several reaction steps and eventually is followed by other reactions obeying the gross reaction scheme

$$C_nH_m + CH_2 \rightarrow C_{n+1}H_{m+2} \tag{4}$$

seem to apply. In addition we note that a significant amount of the consumed methane is deposited as a thin film on the electrodes,[19] most likely as amorphous a:C−H films.

Formation of the small C_2H_m ($m = 2$, 4, 6) hydrocarbons has been investigated in some detail. These hydrocarbons are formed with large probability (Figures 7 and 8). Over the investigated time range, the C_2H_m concentration first increases and, after reaching a maximum concentration, shows a beginning tendency to decrease. This observation may serve as an indication that C_2H_m molecules serve as intermediate steps for formation of larger hydrocarbons. As the dominant species appears the unsaturated C_2H_4 ($m/z = 28$) rather than the saturated C_2H_6 ($m/z = 30$) hydrocarbon. It has to be noted, however, that the fragmentation pattern of C_2H_6 predominately produces a $m/z = 28$ peak making a proper assignment rather difficult (see Table 1).

B. CH_4/N_2. Figure 9 displays the difference spectrum for mass numbers up to $m/z = 40$ on a linear scale obtained by subtracting the data of Figure 2a from those of Figure 2b. As for the

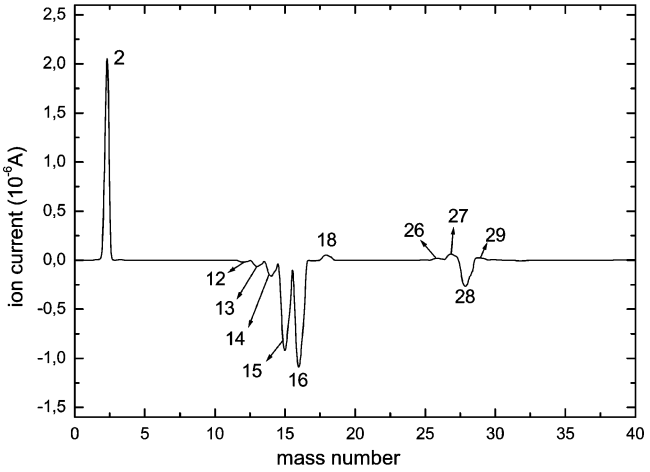

Figure 9. Difference mass spectrum with and without plasma in the mass range m/z up to 40 for a CH_4/N_2 gas mixture. Note the linear scale.

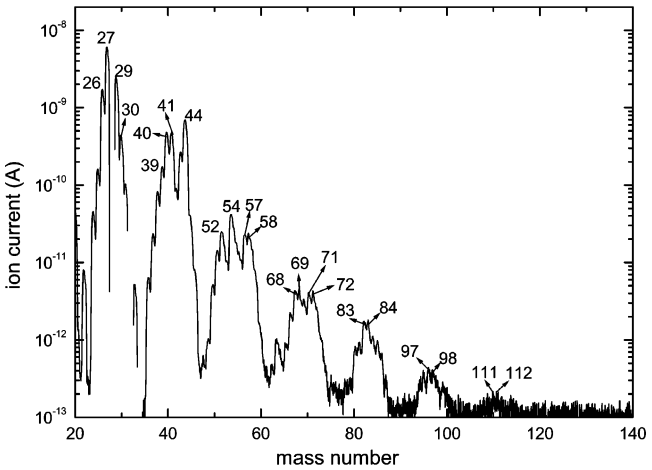

Figure 10. Difference mass spectrum with and without plasma in the mass range $m/z = 20-140$ for a CH_4/N_2 gas mixture.

CH_4/Ar gas mixture, the production of a large amount of hydrogen (H_2) and a significant consumption of methane is evident. The difference spectrum in the mass range $m/z = 20-140$ is displayed in Figure 10 on a logarithmic scale. Again, the broad prominent peaks, each composed of several individual peaks, are attributed to C_nH_m molecules with n up to 8. In addition, consumption of N_2 is noted which may give rise to the formation of HCN ($m/z = 27$) and its CN ($m/z = 26$) fragment. As the $m/z = 26$ and 27 peaks overlap with C_2H_2 and C_2H_3, respectively, no unambiguous identification was possible.

The time dependency of the hydrogen and methane peaks is shown in Figure 11. A similar behavior compared to CH_4/Ar mixture, i.e., a pronounced increase of the hydrogen peak, and an approximately exponential decay of the summed methane peaks ($m/z = 12-16$) is noted. Again, a significant amount of the consumed methane is deposited as a yellowish brown film of a relatively hard material on the electrodes.[19] Preliminary investigations employing X-ray photoelectron and infrared spectroscopy techniques indicate that the deposited film is composed of carbon and nitrogen roughly in a ratio of 2:1 and also contains a significant amount of hydrogen. The details of CN film deposition shall be published elsewhere.

C. Comparison of Ar/CH_4 and N_2/CH_4 Plasmas. Some particular differences between the CH_4/Ar and N_2/CH_4 plasmas

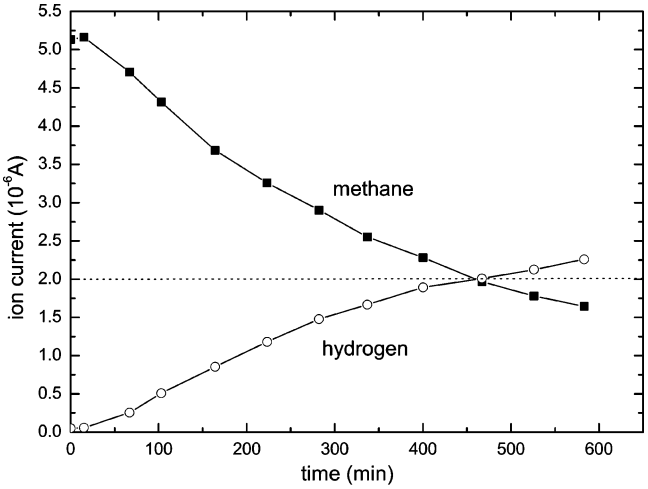

Figure 11. Time dependence of the hydrogen ($m/z = 2$) and methane ($m/z = 12-16$) peaks in the N_2/CH_4 gas mixture.

are worth to be noted. Formation of larger C_nH_m molecules is less probable in CH_4/N_2 compared to CH_4/Ar. This is particularly noticeable for the $n = 9$ peaks which are no longer present in the mass spectrum from CH_4/N_2, as are the larger alkane molecule C_6H_{14} ($m/z = 86$), C_7H_{16} ($m/z = 100$), C_8H_{18} ($m/z = 114$), and C_9H_{20} ($m/z = 128$) and the molecules at $m/z = 78$ and 92 that are hardly or not at all observed. Additional mass peaks occur at $m/z = 52$, 54, 68, 69, 83, 84, 97, 98, 111, and 112; as possible assignments we mention some nitrogen-containing molecules such as cyanogen (C_2N_2, $m/z = 52$), propanenitrile (C_3H_5N, $m/z = 54$), 1-isocyano-propane and 2-methyl-propanenitrile (C_4H_7N, $m/z = 68$ and 69), aziridine ($C_6H_{11}N$, $m/z = 97$), and quinuclidine and exo-2-aminonorbornane ($C_7H_{13}N$, $m/z = 111$).

As was mentioned before, the ion mass spectrum from N_2/CH_4 plasma (Figure 10) drops off more rapidly in comparison to Ar/CH_4 (Figure 6). As both mass spectra were taken under except for the N_2 or Ar gas ad-mixture comparable conditions, we have to conclude that N_2 apparently leads to some "poisoning" of the reaction pathway for the formation of higher order hydrocarbon molecules. The difference may be partly explained by the fewer number of free bonds to which radicals may attach and the more stable chemical bonds formed by nitrogen in comparison to carbon.

V. Discussion

Starting from a pure CH_4 plasma, H_2, C_2H_2, C_2H_4, and CH_4 are the most abundant stable species (Figures 5 and 6). Production of H atoms and H_2 molecules, starts right at the beginning, e.g., by electron impact fragmentation of CH_4,

$$e^- + CH_4 \rightarrow e^- + \begin{Bmatrix} CH_3 + H \\ CH_2 + H_2 \\ CH + H + H_2 \\ C + 2H_2. \end{Bmatrix} \quad (5)$$

According to a widely accepted picture, C_2H_m ($m = 2, 4, 6$) formation in CH_4-containing plasmas is believed to take place in sequential steps,[6,20] i.e.,

$$CH_4 \rightarrow C_2H_6 \rightarrow C_2H_4 \rightarrow C_2H_2. \quad (6)$$

The gas-phase chemistry model of Riccardi et al.[16] favors a different scheme. Using the model outlined in section III we

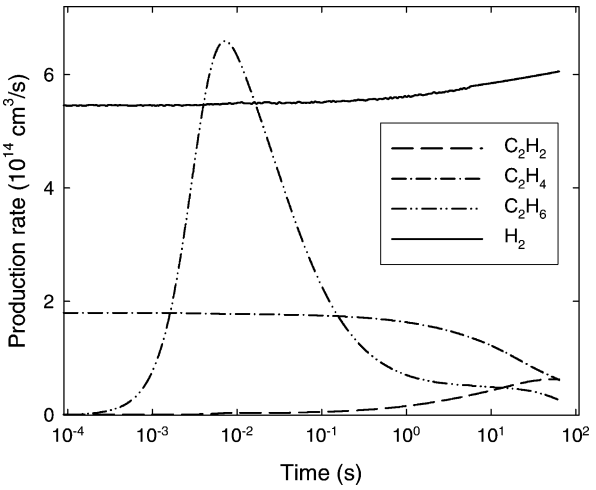

Figure 12. Calculated rates for production of H_2, C_2H_2, C_2H_4, and C_2H_6 in CH_4-containing plasmas.

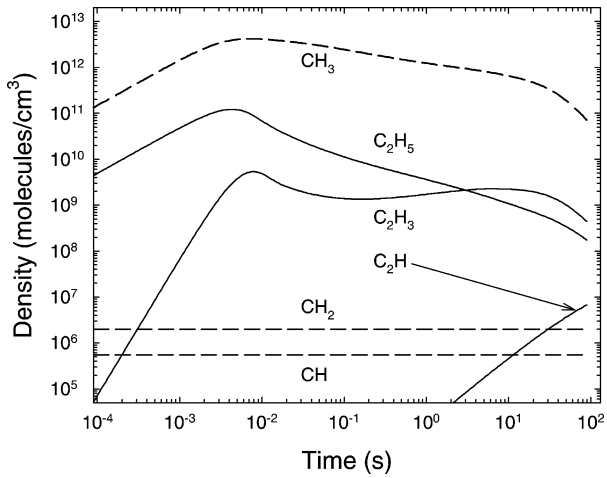

Figure 13. Calculated densities of CH, CH_2, CH_3, C_2H, C_2H_3, and C_2H_5 radicals versus time in CH_4-containing plasmas.

have calculated the production rates and densities of various reaction products in CH_4 plasmas. Due to lacking electron density and temperature measurements, we represent the full temporal dynamics as simplest approximation by a constant electron density $n_e = 10^{12}/m^3$.

Due to the small kinetic energy and mobility of molecules the time scale for chemical reactions to take place is much longer compared to electron reaction times. We thus considered it justified to use time and space averaged values of the electron density, i.e., a mean electron density of $10^{12}/m^3$, in agreement with estimations based on the collected charge and an estimated electron transient time of 10 ns. For the electron temperature the value $T_e = 1$ eV consistent with the transient time estimate was used. As before this is only a crude approximation of the experimental conditions, as more detailed experimental measurements are yet lacking.

For an accurate description of our system a full kinetic model (for example with PIC[14]) is necessary. However, applications of such models to barrier discharge conditions are strongly limited due to run-time limits. On the other hand, simpler fluid models are missing the non-Maxwellian character of the electron energy distribution function. Therefore we decided to stay with a simple zero-dimensional rate equation model to get a first estimate of hydrocarbon pattern in our system.

Our calculated production rates (Figure 12) only partly confirm the reaction scheme of eq 6. The calculations indicate

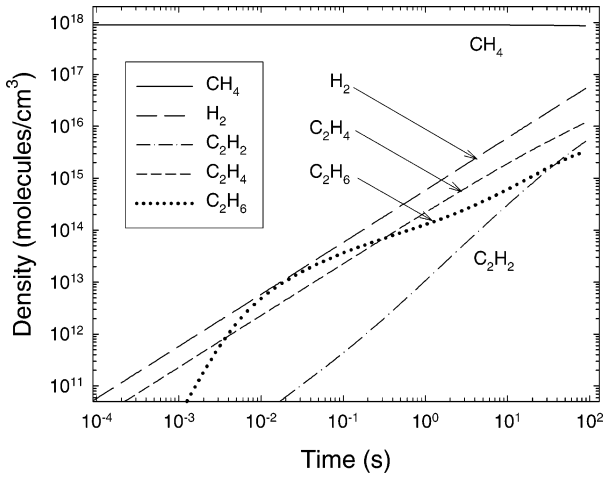

Figure 14. Calculated densities of stable H_2, C_2H_2, C_2H_4, and C_2H_6 molecules versus time in CH_4-containing plasmas.

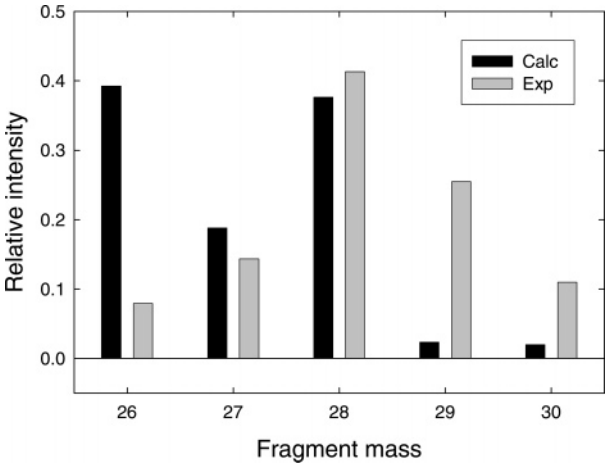

Figure 15. Calculated and measured fragmentation patterns of the C_2H_m peaks ($m = 2-6$) in the CH_4/Ar gas mixture.

that the formed C, CH, CH_2, and CH_3 radicals quickly react to form higher hydrocarbons, e.g.,

$$CH_2 + CH_4 \rightarrow C_2H_4 + H_2 \tag{7}$$

which is the dominant reaction for C_2H_4 production. The main reactions for C_2H_6 formation are

$$CH_3 + CH_3 \rightarrow C_2H_6, \tag{8}$$

which is responsible for the pronounced *overshooting* of the formation rate due to the following rapid depletion of CH_3 radicals, and,

$$C_2H_4 + C_2H_5 \rightarrow C_2H_6 + C_2H_3, \tag{9}$$

which increases with time as more C_2H_4 is formed. Reaction 9, on the other hand, leads to a depletion of C_2H_4 and, hence, is one of the channels responsible for the decrease of the C_2H_4 production rate (Figure 12). The main reactions for C_2H_2 formation are and

$$H + C_2H_3 \rightarrow C_2H_2 + H_2. \tag{10}$$

$$C_2H_4 + C_2H_3 \rightarrow C_2H_2 + C_2H_5. \tag{11}$$

Figure 15 displays the measured pattern of C_2H_m fragments in comparison with our calculated fragmentation pattern. In

contrast to the theoretical data showing pronounced variations the experimental fragmentation pattern varies little with time *t*. To facilitate comparison, we display experimental and theoretical data corresponding to an approximately equal H_2/CH_4 ratio, i.e., experimental data at $t \approx 120$ min from Figure 8 in comparison with theoretical data at $t = 90$ s from Figure 14. The time difference partly reflects the difference in the plasma volume to the chamber volume. It is noted that experimentally the heavier fragments $m/z = 29$ and 30 dominate over the lighter fragments $m/z = 25$ and 26, while our calculations predict just the opposite. Similarly, the calculations of Riccardi et al. favor production of C_2H_2 and C_2H_4 only. The present observation indicates that production of C_2H_2 and C_2H_4 molecules is less likely than predicted theoretically. It should be emphasized that the extent to which the underlying reaction chains actually happen will depend, among other parameters, on the electron temperature, the density, and on the stability of the involved hydrocarbons with respect to chemical reactions. As these parameters are different for experiment and theory some discrepancy appears realistic. Nevertheless, it appears that the general picture of, e.g., C_2H_2 formation in CH_4-containing plasmas is not fully understood yet and that more theoretical and experimental work is needed to clarify the important points.

VI. Summary

The study focuses on the break down properties of CH_4/Ar and CH_4/N_2 plasma in a dielectric barrier discharge. A pronounced break-up of CH_4 molecules and the formation of H_2 molecules is observed. In addition, higher order hydrocarbons C_nH_m with *n* up to 9 and nitrogen-containing hydrocarbon molecules are formed. A limited comparison between experiment and theoretical calculations has been made showing some discrepancies that should be investigated further.

Acknowledgment. We are thankful to Dr. Hartmut Steffen, Axel Knuth, Daniel Köpp, and Jana Kredl for help in building up the experimental set up. Thanks to Dr. H-E Wagner and his group for valuable discussions. Financial support by the International Max-Planck Research School "Bounded Plasmas" (A.M.), the Initiative and Networking Fund of the Helmholtz Association (K.M. and R.S.), and by the Deutsche Forschungsgemeinschaft through Sonderforschungsbereich SFB/TR 24 "Fundamentals of Complex Plasmas" is gratefully acknowledged.

References and Notes

(1) Kogelschatz, U.; Salge, J. In *Low-Pressure Plsma Physics*; Hippler, R., Pfau, S., Schmidt, M., Schoenbach, K. H., Eds.; Wiley-VCH: New York, 2001, p 331.

(2) Samoilovich, V. G.; Gibalov, V.; Kozlov, K. V. *Physical Chemistry of the Barrier Discharge*; Conrads, J. P. F., Leipold, F., Eds.; DVS−Verlag: Dusseldorf, 1997.

(3) Roth, J. R.; Tsai, P. P.-Y.; Wadsworth, L. C. US Patent No. 5,-403,453, 1995.

(4) Basner, R.; Foest, R.; Schmidt, M.; Hempel, F.; Becker, K. *Proceedings of XXIII International Conference on Phenomena in Ionized Gases*, Toulouse, France, July 17−22, 1997, Vol IV, p 196, 1997. Basner, R.; Foest, R.; Schmidt, M.; Hempel, F.; Becker, K. *Gaseous Dielectric*; Christophotou, L. G., James, D. R., Eds., Plenum: New York, 1998; Vol. VIII, p 161.

(5) Sonnenfeld, A.; Tun, T. M.; Zajíčková, L.; Kozlov, K. V.; Wagner, H.-E.; Behnke, J. F.; Hippler, R. *Plasma Polym.* **2002**, *6*, 237.

(6) Kozlov, K. V.; Michel, P.; Wagner, H.-E. *Plasmas Polym.* **2000**, *5*, 129.

(7) Liu, C.-J.; Xue, B.; Eliasson, B.; He, F.; Li, Y.; Xu, G.-H. *Plasma Chem. Plasma Process.* **2001**, *21*, 301.

(8) Kozlov, K. V.; Michel, P.; Wagner, H.-E. *Czech. J. Phys.* **1998**, *48*, 1199.

(9) e.g., Thompson, W. R.; Henry, T. J.; Schwartz, J. M.; Khare, B. N.; Sagan, C. *Icarus* **1991**, *90*, 57; Cravens, T. E.; Vann, J.; Clark, J.; Yu, J.; Keller, C. N.; Brull, C. *Planet. Space Sci.* **2004**, *33*, 212; Waite, J. H.; Niemann, H.; Yelle, R. V.; Kasprzak, W. T.; Cravens, T. E.; Luhmann, J. G.; McNutt, R. L.; Ip, W. H.; Gell, D.; De La Haye, V.; Müller-Wordag, I.; Magee, B.; Borggren, N.; Ledvina, S.; Fletcher, G.; Walter, E.; Miller, R.; Scherer, S.; Thorpe, R.; Xu, J.; Block, B.; Arnett, K. *Science* **2005**, *308*, 982.

(10) Michel, P.; Miethke, F.; Rutscher, A.; Sonnenfeld, A.; Wagner, H.-E.. In *Contributed Papers of 5th International Symposium on High-Pressure Low-Temperature Plasma Chemistry (Hakone V)*; Milovy (Czech Republic), p 52, 1996.

(11) Wagner, H. E.; Brandenburg, R.; Kozlov, K. V.; Sonnenfeld, A.; Michel, P.; Behnke, J. F. *Vacuum* **2003**, *71*, 417.

(12) Boufendi, L.; Bouchoule, A. *Plasma Sources Sci. Technol.* **1994**, *3*, 262.

(13) Boufendi, L.; Hermann, J.; Bouchoule, A.; Dubreuil, B.; Stoffels, E.; Stoffels, W. W.; de Giorgi, M. L. *J. Appl. Phys.* **1994**, *76*, 148.

(14) Matyash, K.; Schneider, R.; Bergmann, A.; Jacob, W.; Fantz, U.; Pecher, P. *J. Nucl. Mat.* **2003**, *434*, 313−316.

(15) Ehrhardt, A. B.; Langer, W. D. *Collisional Processes of Hydrocarbons in Hydrogen Plasmas*; Report PPL-2477, Plasma Physics Laboratory: Princeton University, Princeton, NJ, 1988.

(16) Riccardi, C.; Barni, R.; Fontanesi, M.; Tosi, P. *Czech. J. Phys.* **2000**, textbf 50/S3, 389.

(17) Herrebout, D.; Bogaerts, A.; Yan, M.; Gijbels, R.; Goedheer, W.; Dekempeneer, E. *J. Appl. Phys.* **2001**, *90*, 570.

(18) NIST Standard Reference Database 69 (June 2005), http://webbook.nist.gov/chemistry/.

(19) Yu, K. M.; Cohen, M. L.; Haller, E. E.; Hansen, W. L.; Liu, A. Y.; Wu, I. C. *Phys. Rev.* **1994**, *B49*, 5034.

(20) Kim, S.-S.; Lee, H.; Na, B.-K.; Song, H. K. *Korean J. Chem. Eng.* **2003**, *20*, 869.